Continental Shelf Research 29 (2009) 292–301

Contents lists available at ScienceDirect

Continental Shelf Research

journal homepage: www.elsevier.com/locate/csr

The Columbia River plume as cross-shelf exporter and along-coast barrier

N.S. Banas *, P. MacCready, B.M. Hickey

School of Oceanography, University of Washington, Box 355351, Seattle, WA 98195, USA

ARTICLE INFO

Available online 20 March 2008

Keywords:
Coastal upwelling
River plumes
Columbia River
Numerical modeling
Lagrangian methods
Pacific Northwest
California Current system

ABSTRACT

An intensive Lagrangian particle-tracking analysis of the July 2004 upwelling period was conducted in a hindcast model of the US Pacific Northwest coast, in order to determine the effect of the Columbia River plume on the fate of upwelled water. The model, implemented using Regional Ocean Modeling System (ROMS), includes variable wind and atmospheric forcing, variable Columbia river flow, realistic boundary conditions from Navy Coastal Ocean Model (NCOM), and 10 tidal constituents. Model skill has been demonstrated in detail elsewhere [MacCready, P., Banas, N.S., Hickey, B.M., Dever, E.P., Liu, Y., 2008. A model study of tide- and wind-induced mixing in the Columbia River estuary and plume. Continental Shelf Research, this issue, doi:10.1016/j.csr.2008.03.015]. Particles were released in the Columbia estuary, along the Washington coastal wall, and along the model's northern boundary at 48°N. Particles were tracked in three dimensions, using both velocities from ROMS and a vertical random displacement representing turbulent mixing. When 25 h of upwelling flow is looped and particles tracked for 12 d, their trajectories highlight a field of transient eddies and recirculations on scales from 5 to 50 km both north and south of the Columbia. Not all of these features are caused by plume dynamics, but the presence of the plume increases the entrainment of inner-shelf water into them. The cumulative effect of the plume's interaction with these transient features is to increase cross-shelf dispersion: 25% more water is transported laterally past the 100 m isobath when river and estuarine effects are included than when they are omitted. This cross-shelf dispersion also disrupts the southward transport of water along the inner shelf that occurs in the model when the Columbia River is omitted. This second effect—increased retention of upwelled water on the Washington shelf—may be partly responsible for the regional-scale alongcoast gradient in chlorophyll biomass, although variations in shelf width, the Juan de Fuca Eddy to the north, and the intermittency of upwelling-favorable winds are likely also to play important roles.

1. Introduction

Along the US West Coast, a mean gradient in phytoplankton biomass can be observed that runs counter to the coast-wide gradient in wind stress that drives coastal upwelling (Ware and Thomson, 2005; Thomas et al., 2001; Thomas and Brickley, 2006). This is true in the US Pacific Northwest as along the West Coast as a whole. Phytoplankton biomass is generally higher off Washington than off Oregon, in broad spatial and temporal averages, despite the fact that mean upwelling-favorable wind stress is three times higher off Oregon (Ware and Thomson, 2005; Hickey and Banas, 2003). This paper uses the regional circulation model developed by MacCready et al. (2008), to suggest that the Columbia River plume may play a role in creating this pattern.

Southward (upwelling-favorable) wind stress predominates along the Washington–Oregon coast in summer (Fig. 1), drawing surface waters offshore through Ekman transport and bringing saltier, colder, nutrient-rich water to the surface at the coastal wall (Hickey and Banas, 2003). These nutrients release the phytoplankton population from nitrogen limitation and fuel blooms. Under upwelling-favorable conditions, the Columbia River plume tends southward and offshore, with new fresh water pulsed out of the Columbia estuary on every ebb tide (Fig. 1; Horner-Devine et al., 2008).

Upwelling on the Northwest coast is highly time-dependent. Events in which the large-scale winds not only relax but actively reverse are common throughout the year. Under northward wind (downwelling-favorable) conditions, the Columbia River plume tends northward and onshore along the Washington coast, but within 1–2 d of a return to upwelling-favorable conditions, the plume rapidly advects offshore. Hickey et al. (2005) have shown that because of these wind reversals, there is almost always some amount of plume water off Washington year-round: the summertime Columbia plume should be thought of as bidirectional. In other words, the most typical summer conditions in this region are not "upwelling-favorable" per se, but rather

* Corresponding author. Tel.: +1 206 221 4402.
E-mail address: neil@ocean.washington.edu (N.S. Banas).

0278-4343/$ - see front matter © 2008 Elsevier Ltd. All rights reserved.
doi:10.1016/j.csr.2008.03.011

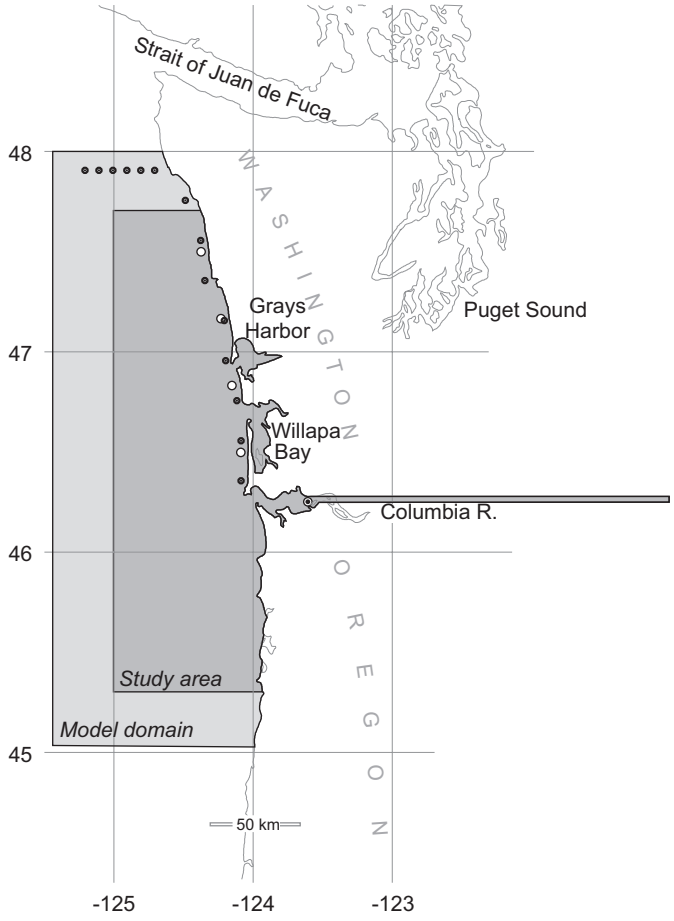

Fig. 1. Full model domain and study area. Launch locations for continuous-release model particles (Figs. 2, 4–7) are shown as open circles, and launch locations for looped-flow particles (Fig. 3) as solid dots.

"upwelling-favorable with a downwelling event a few days in the past."

The Columbia plume may modulate the biological response to upwelling in many ways: by supplying additional nutrients from the Columbia watershed; by entraining additional oceanic nutrients through estuarine or tidal dynamics (Lohan and Bruland, 2006); or by stratifying shelf waters and increasing offshore turbidity, thus altering the availability of light and nutrients over a broad area. In the present study, however, we will consider the plume only as a set of mixing and transport features. Explicit incorporation of plankton community dynamics into the MacCready et al. (2008) model is in progress but beyond the scope of this paper. Our central question is, *What happens to Washington shelf waters (and the nutrients and plankton communities in them) when they encounter the Columbia River plume travelling south under upwelling conditions?* Are they rapidly entrained? If so, does the plume increase or decrease their retention on the shelf? Do shelf waters simply subduct under the plume and continue southward? Do remnants of downwelling plumes on the Washington shelf play an important role?

In the next section, we describe an intensive Lagrangian analysis of one upwelling event in the MacCready et al. (2008) model. Model cases with and without the Columbia River included are considered. The results (Section 3), in brief, suggest that the Columbia River plume is an export feature in the cross-shelf direction but a barrier and retention feature in the along-shelf direction. These alterations of summer circulation patterns are likely to contribute to the large-scale north-to-south gradient in biomass alluded to above.

2. Methods

2.1. The model

MacCready et al. (2008) describe the circulation model used in this study in detail, and also present a much more thorough validation of its velocity and salinity predictions than our results below contain. Only key points are repeated here. The model is implemented using ROMS (Rutgers version 2.2: Haidvogel et al., 2000). The model uses a finite-difference scheme in the horizontal and a generalized, irregularly spaced S-coordinate in the vertical. The turbulence closure is GLS (Generic Length Scale: Umlauf and Burchard, 2003) with Canuto A stability functions (Canuto et al., 2001). The model domain is shown in Fig. 1. Horizontal resolution is ~500 m at the mouth of the Columbia, telescoping out to ~7 km at the northwestern and southwestern corners. The Columbia River beyond a point 50 km upstream of the mouth is replaced by a straight 3 km wide, 3 m deep channel, to allow tidal energy to propagate freely past the estuary. Grays Harbor and Willapa Bay are both included as riverless embayments (Fig. 1): their combined river input is <2% of the Columbia's (Hickey and Banas, 2003).

A 3-month hindcast of June–August 2004 was performed, using time-varying atmospheric forcing, variable riverflow, and tides. Hourly wind and atmospheric forcing is taken from the 4 km Northwest Modeling Consortium MM5 regional forecast model (Mass et al., 2003); daily Columbia river flow is taken from USGS gauge 14246900 at Beaver Army Station (http://waterdata.usgs.gov/or/nwis/); and 10 tidal constituents from the TPXO6 analysis (Egbert et al., 1994; Egbert and Erofeeva, 2002) are applied as surface height and depth-averaged velocity boundary conditions. Boundary conditions for tracers, subtidal velocity, and subtidal surface height come from the NCOM CCS model (Navy Coastal Ocean Model, California Current System: Barron et al., 2006; Kara et al., 2006). In general, the MacCready et al. model reproduces time series of velocity, salinity, and temperature at three mid-shelf locations with correlation coefficients ~0.5 during the time period analyzed here: details can be found in MacCready et al. (2008).

2.2. Particle tracking numerics

Particles were tracked entirely in postprocessing, using custom Java code that integrates 3D velocity fields from ROMS saved every lunar hour (3726 s). A fourth-order Runge–Kutta scheme was used for the integration, with a timestep of 300 s. In addition to advection in all three dimensions, particles were subject to vertical diffusion, using the "random displacement" scheme described by Visser (1997; see also Batchelder et al., 2002; Brickman and Smith, 2002). This scheme adds a random vertical velocity, scaled by the local vertical diffusivity from ROMS, to the advective velocity at every timestep, and also includes a correction based on the local diffusivity gradient:

$$z_{n+1} = z_n + \Delta t\left(w_{\mathrm{adv}} + R\sqrt{\frac{2\kappa}{\Delta t}} + \frac{\partial \kappa}{\partial z}\right) \quad (1)$$

where z is vertical position, Δt the timestep, w_{adv} the advective velocity, R a normally distributed random function with mean 0 and variance 1, and κ the vertical diffusivity. Following Batchelder et al. (2002), $\partial\kappa/\partial z$ is evaluated at $z_n + w_{\mathrm{adv}}\Delta t$ and κ is evaluated at $z_n + \Delta t(w_{\mathrm{adv}} + 1/2\ \partial\kappa/\partial z)$.

The gradient correction is essential to preventing particles from accumulating unrealistically in low-diffusivity areas, as demonstrated vividly by Visser (1997). A first-order correction as in (1) is valid only if the integration timestep is sufficiently short:

$$\Delta t \ll \left(\max\left(\frac{\partial^2 \kappa}{\partial z^2} \right) \right)^{-1} \quad (2)$$

(Visser, 1997). If $\partial^2\kappa/\partial z^2$ were evaluated locally on the model grid, then the vertical grid spacing would place a drastic limit on the integration timestep ($\Delta t < 1$ s in the Columbia estuary, where surface sigma layers are <1 cm thick). Such an approach, however, places unrealistic importance on the details of the ROMS diffusivity parameterization, and so instead we rearrange (2) into an expression for the length scale Δz over which the diffusivity profile should be smoothed to match our chosen timestep. If $\partial^2\kappa/\partial z^2 \approx \kappa/\Delta z^2$, then

$$\Delta z \gg \sqrt{\max(\kappa)\Delta t} \approx 0.5\, m \quad (3)$$

For safety, we evaluate $\partial\kappa/\partial z$ in Eq. (1) over a slightly longer span, 2 m. (There is no reason to believe our model accurately captures diffusivity variation on smaller scales than this anyway, and results do not appear to be sensitive to this choice of length scale.) A reflective top and bottom boundary condition was used, following North et al. (2006).

2.3. Particle tracking experiments

Two model scenarios are considered in this study, in order to isolate the effects of the Columbia River plume from the equally complex flows caused by topography and variable winds. The first (the "River case") is as described above, forced by winds, tides, and variable Columbia riverflow, with the Columbia estuary, Willapa Bay, and Grays Harbor included. In the second case ("No Estuary"), riverflow is set to zero and the mouths of the three estuaries are sealed off in the model grid, so that the coastline is unbroken.

Two types of particle experiments were conducted in each of these model scenarios. "Continuous release" particles were launched once per tidal hour (3726 s) at four locations on the Washington coast and in the Columbia estuary (Fig. 1, open circles), starting June 18 and ending August 16, 2004: 6855 releases total. Each particle was tracked for 20 d. These are the trajectories upon which our statistical results are based (Section 3.3 below).

These trajectories are difficult to interpret mechanistically, however, because of the variety of wind conditions experienced by each particle. To address this, we also conducted two "looped-flow" experiments, in which particles were tracked for 12 d, but in a partially artificial flow field: one tidal day (24.84 h) of flow from ROMS was looped, as if July 23 or July 26, 2004 occurred 12 times in a row. July 23 and 26 were chosen because they fall at the beginning and in the middle of a sustained upwelling event (see Fig. 2a): they can thus be thought of as "typical" upwelling days. Columbia flow volume was close to the seasonal mean during this period as well (MacCready et al., 2008). Looped-flow particles were released at 7 locations along the northern model boundary (in the vicinity of the Juan de Fuca eddy: MacFadyen et al., 2005), 8 locations along the Washington coastal wall, and in the Columbia estuary. At each location, 10 particles were released each tidal hour, for a total of 3840 per experiment.

This strategy of looping 1 day of flow is a negotiation between two concerns. On the one hand, transients are essential to this system, as described in the Introduction. If we had, say, run the model to a true steady state under constant upwelling winds, the plume would be unidirectional, not bidirectional (Hickey et al., 2005), and therefore the modeled Washington coastal circulation would be even farther from "typical" upwelling than in the artificial looped-flow scenario. On the other hand, tracking particles through an actual 12 d or longer hindcast of any particular period would conflate upwelling, downwelling, and weak-wind circulation in idiosyncratic proportions, and obscure the dynamics of any particular day. The hybrid method we have chosen—preserving tidal variability over 25 h but otherwise freezing the circulation mid-wind event—produces trajectories than can be thought of (loosely, heuristically, not quantitatively) as a turbulent, diffusive analog to *streamlines*. These pseudo-streamlines reveal transients whose cumulative importance can be assessed using more the realistic evolving-flow, continous-release trajectories.

In the results that follow, we will first use the looped-flow experiments to illustrate plume-related transport and retention mechanisms that occur under upwelling conditions. Afterwards, we will compare the continuous-release particle results from the River and No Estuary cases in order to quantify the cumulative role of the Columbia River plume.

3. Results

3.1. Behavior of the plume under variable upwelling

A timeline of the July 2004 upwelling period is shown in Fig. 2. Seven 25-h-average snapshots of surface salinity are shown (Fig. 2b), progressing from a strongly bidirectional plume under weak winds (July 17), to a downwelling plume following a northward wind event (July 20), to a south-tending plume under sustained upwelling-favorable winds (July 23–29), and finally back to a strongly bidirectional plume as the wind relaxes (August 1–4). The plume is bidirectional in a weaker sense almost continously throughout this timeline: <31 psu water can be found on the Washington coast in every snapshot but July 26. In particular, on July 23, the dissipating, spreading downwelling plume can be seen as a continuous feature along the Washington coast from the Columbia past Grays Harbor.

Note also that the freshwater seen in Willapa Bay and Grays Harbor in this model is entirely Columbia River derived. The trapping of plume water in the Washington estuaries and its slow release back into the coastal ocean (e.g., Willapa Bay, July 20–23) is consistent with past observations of plume intrusions in these estuaries (Hickey and Banas, 2003; Banas et al., 2004). This is another mechanism by which freshwater and estuarine dynamics cause dispersion on this coast, although we have not quantified it in this study.

Maps of salinity reveal some of the mesoscale mixing and dispersion occurring during this upwelling event, but obscure the history of particular plume water masses. In order to distinguish new plume water that has just left the estuary from aged plume water—a distinction that may not matter to the physics but is crucial to the biology of the system—we can use the time information associated with the continuous-release Columbia estuary particles (see Fig. 1). The ages (time since release) of all particles found in salinity <31.5 psu are shown in Fig. 2c. There is, as one would expect, a general pattern of younger water close to the Columbia mouth and older water farther from it, but perhaps what is most striking is that this age-distance trend is as weak as it is. Even on days when a linear plume axis is clearly defined (like July 23), the water all along that axis is a mixture of new plume water with water that left the estuary up to 15 d before. On August 4, this is dramatically the case even in the near-field plume, 0–20 km from the river mouth. This mixing of ages is one

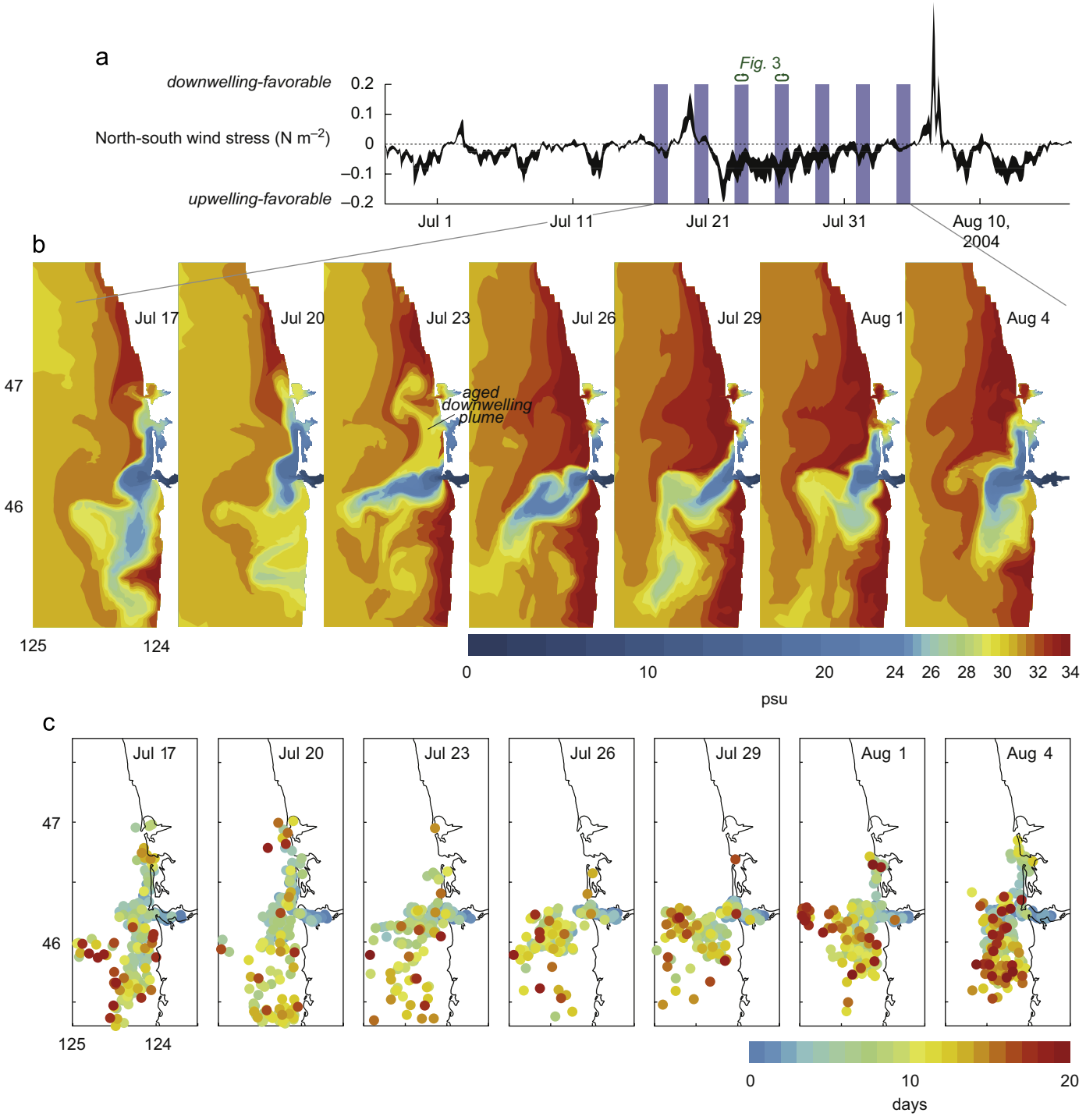

Fig. 2. (a) North–south wind forcing during July and early August 2004. The width of the black line indicates standard deviation in wind stress over the model domain. Blue bars mark the 25 h averages shown in (b) and (c). The July 23 and July 26 looped-flow experiments shown in Fig. 3 are labeled in green. (b) Model surface salinity. (c) Location and age (time since launch) of particles released continuously in the Columbia estuary.

indication that the plume is not simply a conveyor belt or highway from a Lagrangian point of view, but rather a place of retention as much as it is an advective pathway.

3.2. Eddies and retention in the plume region

The timeline above highlights the amount of circulational complexity and "coarse-grained mixing" (Ridderinkhof and Zimmerman, 1992) that even a slow, orderly oscillation between upwelling and downwelling conditions can cause. To identify mechanisms, we need to examine even narrower snapshots in time. A synoptic view of looped-flow particle trajectories from July 23 is shown in Fig. 3a, with key features of the July 26 results shown in insets (Fig. 3c and d). Full 12 d particle paths are shown, but as discussed above, these should be thought of as something akin to streamlines of the tidally averaged circulation, not as trajectories of actual water masses.

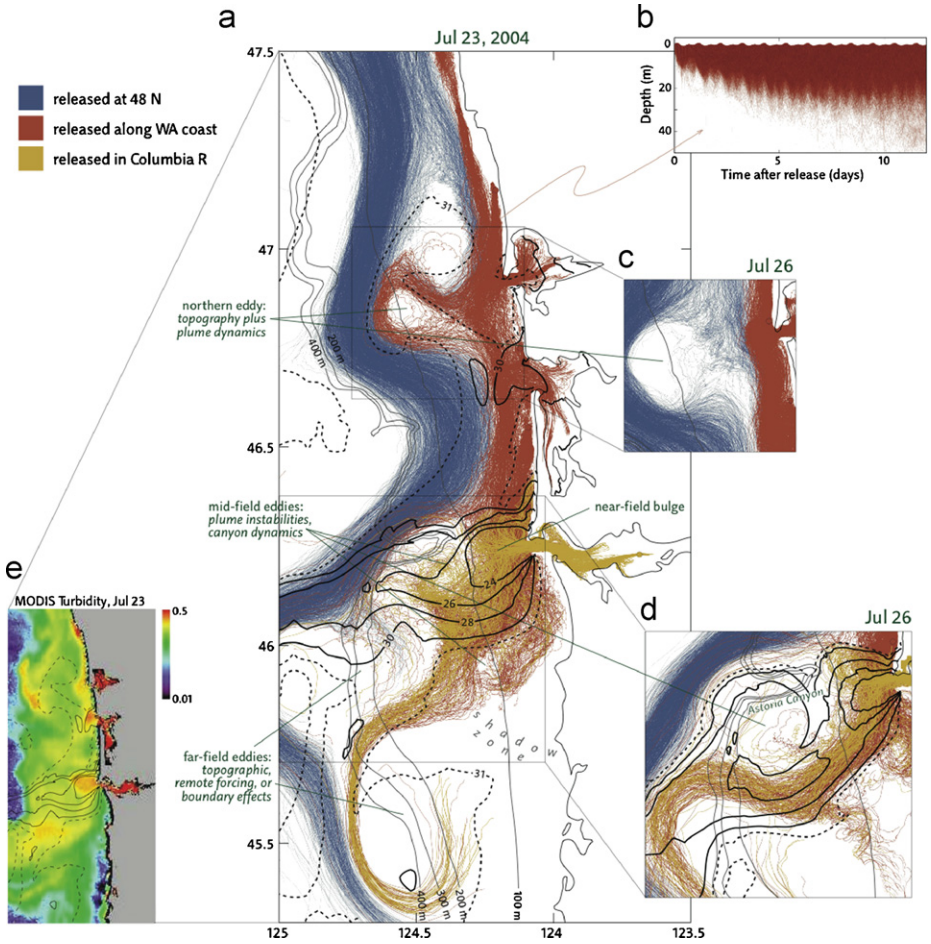

Fig. 3. Looped-flow particle trajectories from July 23 (a) and July 26 (insets c,d). Thin black contours show the bathymetry (100, 200, 300, 400 m) and thick black contours surface salinty (24, 26, 28, 30 psu as solid lines, 31 psi as a dotted line: compare Fig. 2b). The Washington-coast-release particles from July 23 (a, red trajectories) are also shown in a depth-vs.-time plot (b). A satellite image of turbidity from July 23 (courtesy of R. Kudela, http://oceandatacenter.ucsc.edu/RISE/) is also shown (e), with salinity contours from (a) overlaid for comparison.

This depiction of the flow highlights the extent to which the Columbia River plume is made up of eddies and recirculation features. In the literature of river plume dynamics, the rotating bulge that often forms immediately outside the mouth has received thorough attention (Garvine, 1995; Yankovsky, 2000; Fong and Geyer, 2002; Horner-Devine et al., 2008). On July 23 and 26, however, this near-field eddy appears to be just one of several, as we will now discuss in detail.

First, there is a 20-km-wide cyclonic eddy on the outer shelf just south of 47°N ("northern eddy," Fig. 3a and c). On July 23 this eddy is half of a dipole pair associated with the tip of the spreading down-welling plume (31 psu contour; compare Fig. 2b) but this dipole structure appears to be transient. The cyclonic eddy itself, however, is long-lived and recurrent. It lasts past July 26 (Fig. 3c) in the River model case shown here, and, strikingly, persists through this event and much of the summer in the same location in the No Estuary case as well (not shown). Thus it appears to be primarily a topographic effect, associated with the variation in shelf width between 46.5 and 46.7°N (blue trajectories, Fig. 3a). Entrainment of coastal water into this eddy, in contrast, appears to be associated with the plume and highly transitory (red trajectories, Fig. 2a vs. c).

Second, large eddies can be seen in the far-field plume region, on the slope and beyond (Fig. 3a and d). These may be topographic effects associated with changes in shelf width; remotely forced features propagating northward from the larger NCOM CCS domain our model is nested in; or simply model artifacts created by the southern and eastern boundary conditions.

Finally, there is a complex set of small mid-field eddies on the shelf at or below the latitude of the Columbia. Such eddies are thought to form in the Columbia plume, as in other plumes, both through tidal pulsing (Horner-Devine et al., 2008) and through non-tidal, shear-driven mechanisms (Yankovsky et al., 2001; Garcia Berdeal et al., 2002). Upwelling in Astoria Canyon (Hickey, 1997; Fig. 3d) most likely also plays an important role.

We cannot expect a numerical model to capture the details of such complex eddy fields point by point, but a real-world drifter experiment on July 26 confirms, at least, the scale of motion in these mid-field eddies. The trajectories of two drifters released from the R/V Wecoma at 0700 GMT on July 26 are shown in Fig. 4. One (dotted line) is surface-trapped, while the other (solid line) follows a 10 m drogue extending from 15 to 25 m depth. A set of model particles released at the same place and time from 0 to 25 m depth, tracked for 4 d in the evolving (non-looped) model flow, are shown in gray for comparison. The surface drifter rapidly moves south at $>20\,\mathrm{cm\,s^{-1}}$, but neither the drogued drifter nor the model particles do so: for at least 4 d they circulate locally around eddy-like features at speeds $\sim 5\,\mathrm{cm\,s^{-1}}$. Note that because of vertical mixing, all of the model particles in this study spread throughout the upper 20–30 m of the water column within a few

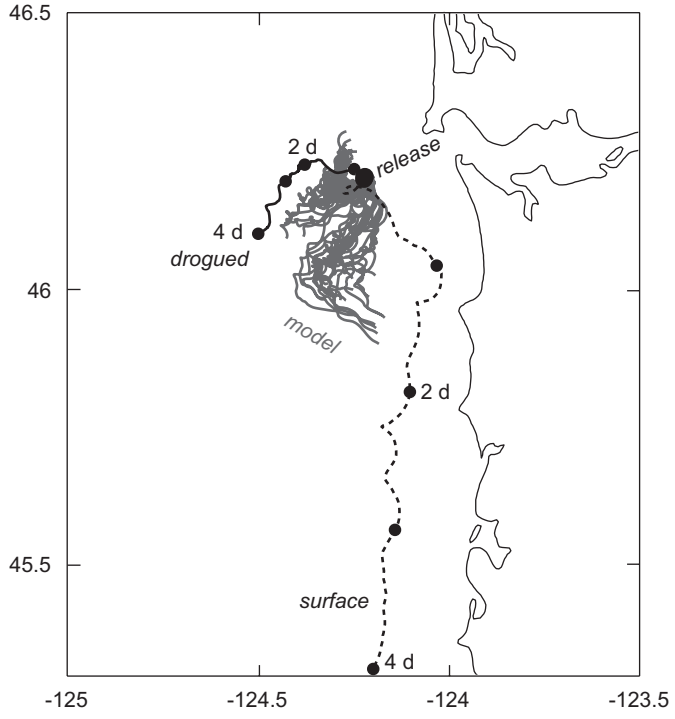

Fig. 4. Trajectories of two real-world GPS-tracked drifters released simultaneously on July 26, one with a 10 m drogue extending from 15 to 25 m (black dotted line) and one surface-trapped (black solid line). Dots mark position at 1 d intervals. Four days model trajectories starting at the same location and time are shown in gray.

days (Fig. 3b). Thus model particles, like the drogued July 26 drifter, effectively average the currents over this depth range as they travel. The striking difference between surface and drogued drifter paths on July 26 demonstrates that the mean flow over 20–30 m may indeed contain retention and recirculation features like the model eddies described above, even if surface currents do not indicate them at all.

To summarize: during upwelling, a variety of eddies formed by a variety of mechanisms can be found in the Columbia plume region. These eddies are co-located with both the northern and southern branches of the plume, but only some of them are *caused* by the plume: in fact it appears that these eddies may *define* the mid- and far-field plume under upwelling conditions. That is, what we call the plume, beyond the near-field bulge, is essentially the set of places where freshwater mixes away most slowly: a map of retention features. Even when these retention features are continguous and form an "axis" of low surface salinity, the principal advective pathway in the plume is not necessarily oriented along the axis, but rather around and between the individual recirculations (Fig. 3d).

Entrainment of recently upwelled water into this eddy field (red trajectories, Fig. 3) appears to be highly episodic (e.g., northern eddy, Fig. 3a and d), but also potentially important on a large scale. On July 23, water parcels (or rather, pseudo-streamlines) from the Washington upwelling zone are very dramatically diverted into the mid-field plume as opposed to continuing south, thus creating a "shadow zone" on the northern Oregon shelf (Fig. 3a). This may be a transient phenomenon—by July 26, trajectories have begun to exit the plume region into this shadow zone (Fig. 3d)—but it does appear to be real. A July 23 satellite image of turbidity, a proxy for recent freshwater influence, is shown in Fig. 3e (courtesy of R. Kudela, http://oceandatacenter.ucsc.edu/RISE/). The low-turbidity region off Oregon is nearly identical in shape and extent to the "shadowed" area, which modeled Washington and Columbia River water are diverted from. This correspondence breaks down only in the far field, over the slope and beyond.

Together these results, albeit anecdotal, suggest a mechanistic hypothesis: The Columbia River plume increases the entrainment of Washington coastal water into shelf and slope eddies: eddies that may be transient or recurrent, driven by plume dynamics or else simply co-located with plume waters. The net effect of this entrainment is to decrease connectivity between the Washington upwelling system and the Oregon shelf. In the next section, we will use the more comprehensive continuous-release particle experiments to confirm this hypothesis and quantify this along-coast retention effect.

3.3. Along-coast dispersion and retention

For context, an overview of continuous-release particle trajectories starting on the Washington coast in the River and No Estuary model cases is shown in Fig. 5. The four coastal launch locations (white dots) and a series of upwelling and downwelling events (Fig. 2a) are conflated in this view, but one can still conclude that in the No Estuary case, trajectories are (1) more tightly confined along the Washington shelf and (2) denser on the northern Oregon inner shelf. Both of these patterns are consistent with the hypothesis stated above.

For a more precise view of net advection and dispersion, the locations after 10 d of particles released at 46.83°N are shown in Fig. 6, in plan view (Fig. 6a) and as a timeline that makes

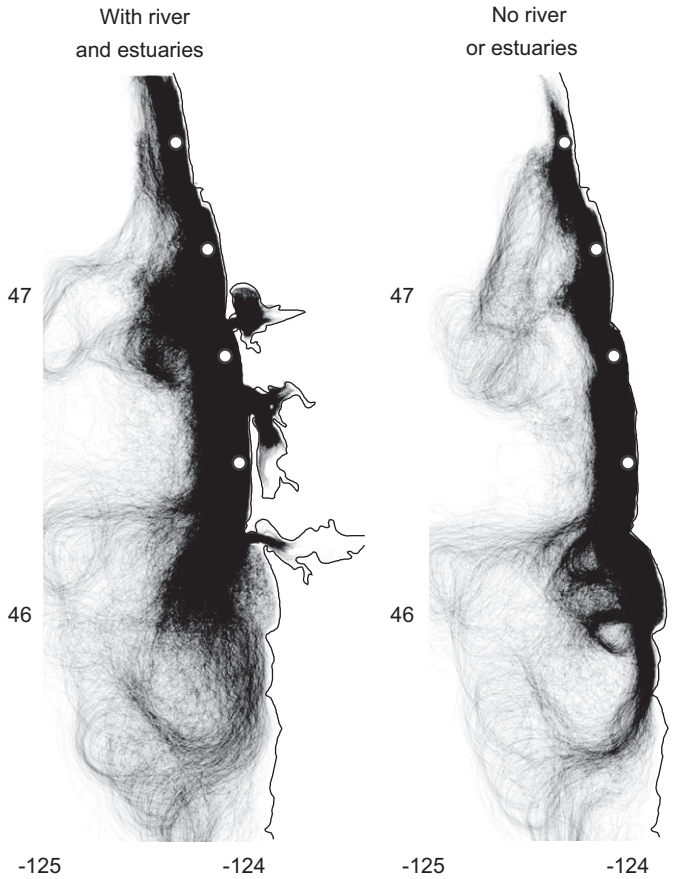

Fig. 5. Overview of all continuous-release particle trajectories beginning at four launch sites on the Washignton coast (white dots; compare Fig. 1) for model cases with and without the Columbia River and Washington estuaries included.

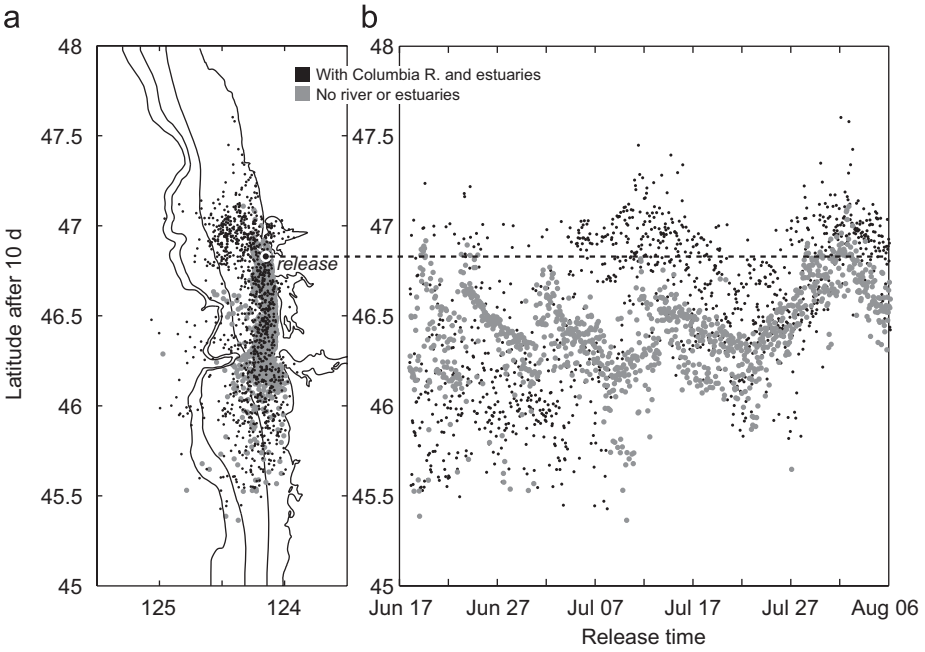

Fig. 6. Location after 10 d of transport of particles released continuously at 46.83°N, in plan view (a) and arrayed by release time (b).

event-scale variation apparent (Fig. 6b). In the average over the entire time period shown, the net latitudinal displacement in the River case (mean ± std dev) is 30 ± 50 km over 10 d, compared with 50 ± 30 km in the No Estuary case. Thus along-coast dispersion is increased in the presence of the plume, while southward advection is reduced. This northward bias in the plume case is equivalent to the "along-coast retention" we hypothesized earlier. The plume also appears to amplify the difference between upwelling and downwelling-favorable conditions: in the presence of the plume, northward net transport during downwelling is much stronger (release times July 9–19 and July 28–August 7; compare wind time series in Fig. 2a).

3.4. Cross-shelf export

The analysis above shows that in the along-coast direction, the dispersion introduced by the Columbia plume has the net effect of decreasing mean transport. In the cross-shelf direction, however, this dispersion process appears to have the opposite effect. In Fig. 7, we have plotted all latitudes and times at which particles launched off Washington (along the 15 m isobath) are found on the Oregon shelf inshore of the 60 m isobath, with ages < 10 d, in both River and No Estuary model cases. This is a measure of the connectivity of the Washington and Oregon upwelling zones, and of cross-isobath retention and export. In the No Estuary case, particles are found to make this Washington-to-Oregon connection under all conditions except the strongest and most sustained upwelling event observed (late July: compare Fig. 2), whereas in the River case this connectivity is more episodic. Overall, connectivity in the presence of the plume is only 27% of what it is in the plume's absence (ratio of black dots to gray dots, Fig. 7).

Furthermore, just as less Washington water is found on the Oregon inner-to-mid shelf in the River case, so also is much more Washington water found on the outer shelf, slope, and beyond. The fraction of Washington inner-shelf water found past the 100 m isobath is shown in Fig. 8 as a function of water age for all four continuous-release launch locations and both model cases (compare Fig. 5). For launch locations within 80 km of the river mouth (46.5 and 46.83°N), export past 100 m after 20 d is increased ~40% in the presence of the plume, although for launch locations farther north (47.17 and 47.5°N) this effect is nonexistent or weakly negative. Thus plume dynamics introduce heterogeneity into the fate of Washington upwelled water (clustered gray lines vs. unclustered black lines, Fig. 8), in addition to increasing cross-shelf export overall. All these results are consistent with the eddy-entrainment mechanisms posited on the basis of the looped-flow analysis.

4. Conclusions

We began with the question, What happens to Washington shelf waters when they encounter the Columbia River plume under upwelling conditions? Analysis of the July 2004 intermittent-upwelling period has yielded the short answer that the plume *disperses* water that upwells off Washington over a very broad area (Fig. 9). The bidirectionality of the Columbia River plume is an essential part of this process: even weak remnants of down-welling plumes can still have important effects on the fate of coastal water on the Washington shelf (Fig. 3). Overall, over 20 d, ~25% more water is exported laterally from the Washington nearshore past the 100 m isobath when the Columbia River plume is included in the model (Fig. 8, average over all release locations). Furthermore, in the first 5–10 d from each water parcel's appearance at the coast—a timescale more relevant to many biological questions—this additional export is 70–100%. One might expect that this increased lateral export into regions of deeper water ultimately causes increased vertical export in the biogeochemical sense, but we cannot quantify the plume's effect on, say, vertical carbon flux any further using this analysis.

The plume is not only a cross-shelf exporter, but a semi-permeable along-shelf barrier as well (Fig. 9). When caught at just the right moment (July 23 or July 26: Figs. 2 and 3), the flow past the Columbia River mouth region looks like something like a headland eddy or coastal jet (Hickey, 1989), although the net effect of the eddy field near the river mouth is more diffuse

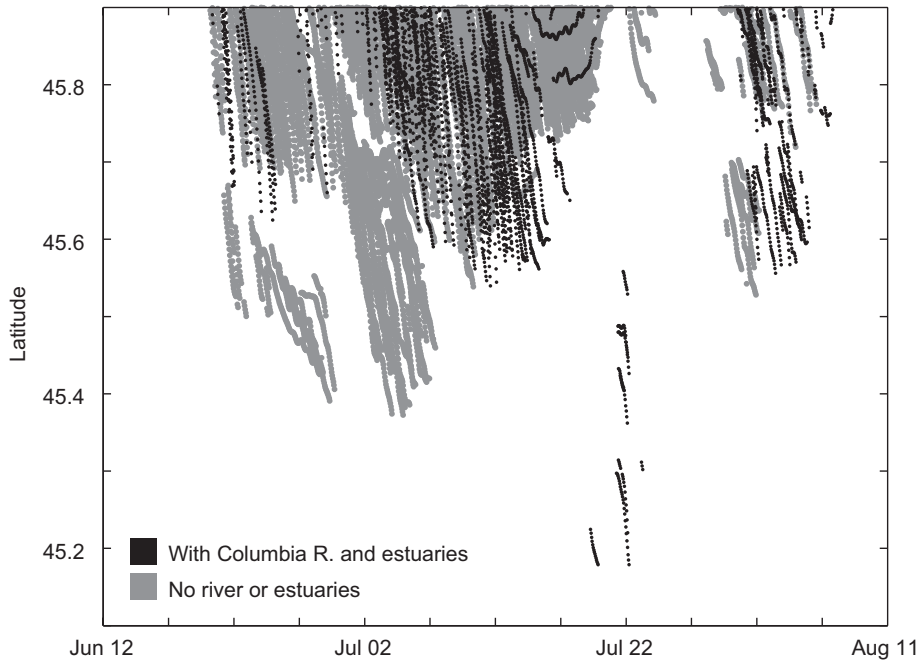

Fig. 7. Latitudes and times at which particles released at Washington-coast locations in Fig. 5 are found inshore of the 60 m isobath off Oregon. The date shown is the date of occurrence off Oregon; particle release times are 0–10 d earlier (particles with age >10 d are not shown). Results are shown for River and No Estuary model cases.

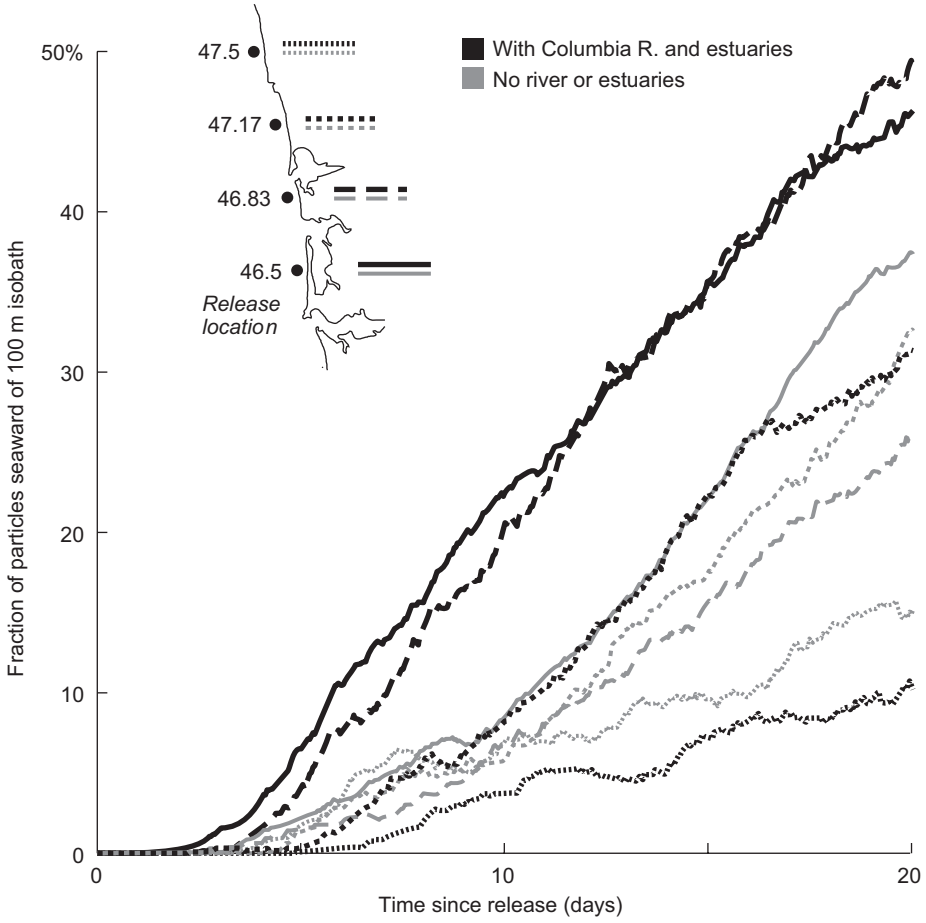

Fig. 8. Fraction of particles released along the Washington coast found seaward of the 100 m isobath, 0–20 d after release. Lines vary from solid to dashed to dotted with latitude. The River (black) and No Estuary (gray) model cases are both shown.

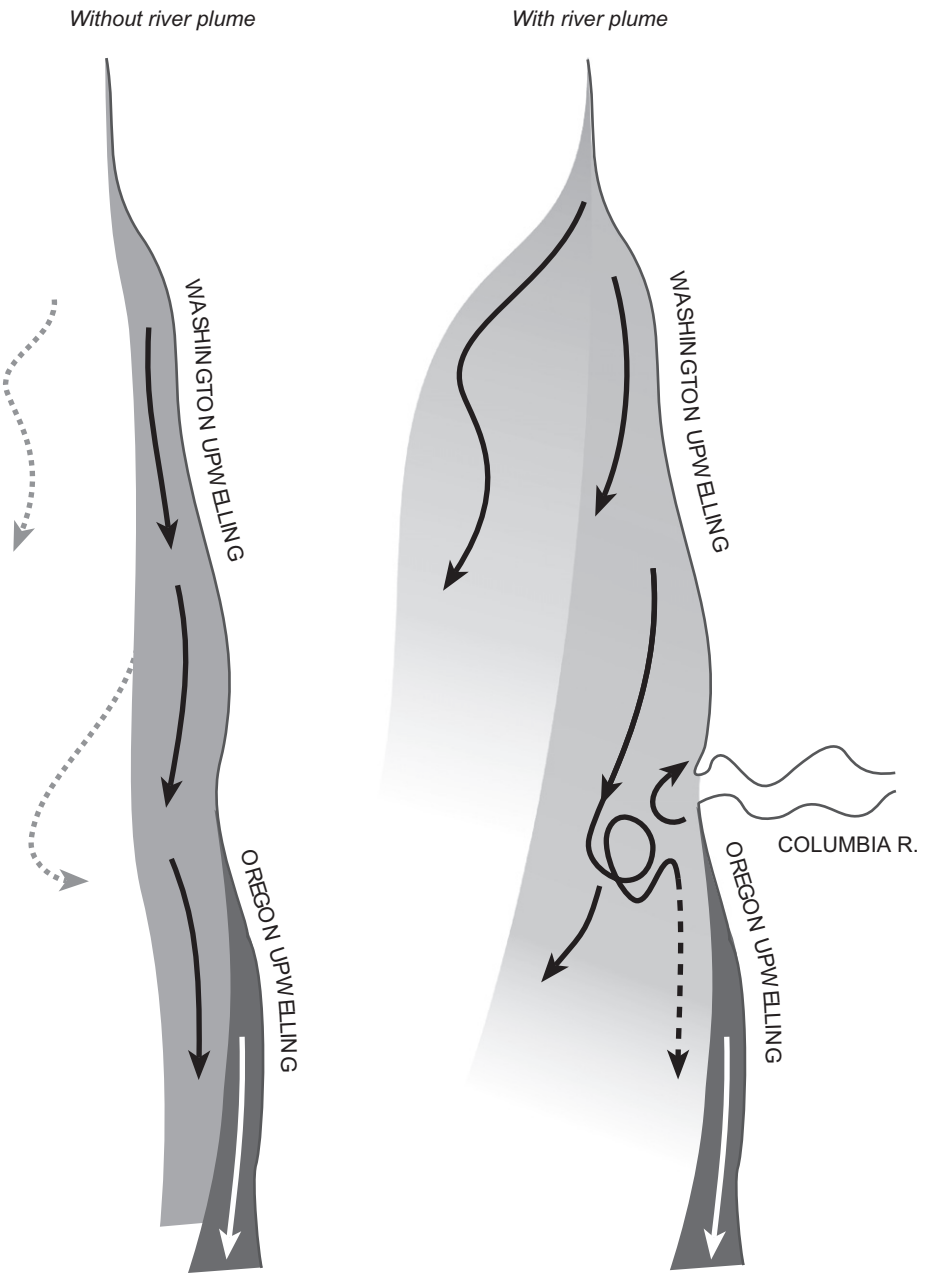

Fig. 9. Schematic of the effect of the Columbia River plume on the fate of upwelled water during events like the late-July 2004 upwelling period considered here. Without the plume (left), water upwelled off Washington advects south along the inner and mid-shelf, merging with the inner-shelf upwelling system off northern Oregon. Some topographic recirculation occurs on the mid-to-outer shelf (dotted lines), but entrainment of newly upwelled water into these features is relatively weak. In the presence of the plume (right), entrainment into such mesoscale features is more common: this increases the dispersion of Washington coastal water onto the outer shelf and slope, and also retards the southward advection of that water along the inner shelf. The input of aged Washington coastal water into the Oregon inner-shelf upwelling zone is thus reduced (but not eliminated: dashed line), as in the lee of some headlands.

(Fig. 5). Still, the plume does cause a net diversion of Washington coastal production away from the inner shelf south of the river mouth (Fig. 7). Thus we expect that the northern Oregon upwelling system "resets" much the way that upwelling centers in the lee of small headlands do (e.g. Roughan et al., 2005; see also Strub et al., 1991; Fig. 9). This pattern could explain why integrated surface chlorophyll off the northern Oregon coast is anomalously low (Ware and Thomson, 2005; Thomas and Brickley, 2006). In this hypothesis, upwelling off northern Oregon only controls biomass in a narrow band along the coast, while the biomass in water farther offshore derives from Washington upwelling and is depleted by age and isolation from near-shore nutrients. In the absence of these plume effects, we would expect greater homogeneity along the coast: a more two-dimensional upwelling system (Fig. 9).

At the same time, the plume is far from the only mechanism introducing heterogeneity into this system. The looped-flow analysis above (Fig. 3) highlights the importance of topographic effects on the flow, on scales from the local effects of Astoria Canyon, Willapa Bay, and Grays Harbor to ~100 km variations in shelf width. Nutrients or biomass advected south from the Juan de Fuca Eddy may also be essential in establishing the Washington–Oregon biomass gradient (MacFadyen et al., 2005). The intermittency of the wind by itself may have important effects

on material exchange (Samelson and Wiggins, 2006, Chapter 5) or patterns of productivity (Botsford et al., 2006). Ultimately a comprehensive modeling approach to the regional biomass-gradient question will require (1) a spatial domain expanded both north and south, and (2) a careful consideration of the timescales of nutrient-phytoplankton-zooplankton interactions in comparison with timescales of export and retention.

Acknowledgments

This work was supported by NSF Grant OCE 0239089. This is contribution #16 of the NSF CoOP RISE (River Influences on Shelf Ecosystems) program. Many thanks to David Darr for his help with model development and system administration, and to Ryan McCabe for deploying the two real drifters discussed and processing the results. Conversations with Jamie Pringle, Elizabeth North, and Antonio Baptista about methods, and with Amy MacFadyen, Raphe Kudela, and Yonggang Liu about regional dynamics, were very helpful.

References

Banas, N.S., Hickey, B.M., MacCready, P., Newton, J.A., 2004. Dynamics of Willapa Bay, Washington: a highly unsteady, partially mixed estuary. Journal of Physical Oceanography 34, 2413–2427.

Barron, C.N., Kara, A.B., Martin, P.J., Rhodes, R.C., Smedstad, L.F., 2006. Formulation, implementation and examination of vertical coordinate choices in the global navy coastal ocean model (NCOM). Ocean Modelling 11, 347–375.

Batchelder, H.P., Edwards, C.A., Powell, T.M., 2002. Individual-based models of copepod populations in coastal upwelling regions: implications of physiologically and environmentally influenced diel vertical migration on demographic success and nearshore retention. Progress in Oceanography 53, 307–333.

Botsford, L.W., Lawrence, C.A., Dever, E.P., Hastings, A., Largier, J., 2006. Effects of variable winds on biological productivity on continental shelves in coastal upwelling systems. Deep Sea Research II 53, 3116–3140.

Brickman, D., Smith, P.C., 2002. Lagrangian stochastic modeling in coastal oceanography. Journal of Atmospheric and Oceanic Technology 19, 83–99.

Canuto, V.M., Howard, A., Cheng, Y., Dubovikov, M.S., 2001. Ocean turbulence. Part I: one-point closure model—momentum and heat vertical diffusivities. Journal of Physical Oceanography 31, 1413–1426.

Egbert, G., Erofeeva, N., 2002. Efficient inverse modeling of barotropic ocean tides. Journal of Atmospheric and Oceanic Technology 19, N2.

Egbert, G., Bennett, A., Foreman, M., 1994. TOPEX/Poseidon tides estimated using a global inverse model. Journal of Geophysical Research 99, 24,821–24,852.

Fong, D.A., Geyer, W.R., 2002. The alongshore transport of freshwater in a surface-trapped river plume. Journal of Physical Oceanography 32, 957–972.

Garcia Berdeal, I., Hickey, B.M., Kawase, M., 2002. Influence of wind stress and ambient flow on a high discharge river plume. Journal of Geophysical Research 107 (C9), 3130.

Garvine, R.W., 1995. A dynamical system of classifying buoyant coastal discharges. Continental Shelf Research 15, 1585–1596.

Haidvogel, D.B., Arango, H.G., Hedstrom, K., Beckmann, A., Malanotte-Rizzoli, P., Shchepetkin, A.F., 2000. Model evaluation experiments in the North Atlantic Basin: simulations in nonlinear terrain-following coordinates. Dynamics of Atmospheres and Oceans 32, 239–281.

Hickey, B.M., 1989. Patterns and processes of circulation over the shelf and slope. In: Hickey, B.M., Landry, M.R. (Eds.), Coastal Oceanography of Washington and Oregon. Elsevier, Amsterdam, pp. 41–115.

Hickey, B.M., 1997. The response of a steep-sides, narrow canyon to time-variable wind forcing. Journal of Physical Oceanography 27, 697–726.

Hickey, B.M., Banas, N.S., 2003. Oceanography of the US Pacific northwest coastal ocean and estuaries with application to coastal ecology. Estuaries 26, 1010–1031.

Hickey, B.M., Geier, S., Kachel, N., MacFadyen, A., 2005. A bi-directional river plume: the Columbia in summer. Continental Shelf Research 25, 1631–1656.

Horner-Devine, A.R., Jay, D.A., Orton, P.M., Spahn, E.Y., 2008. A conceptual model of the strongly tidal Columbia River plume. Journal Of Marine Systems, in press.

Kara, A.B., Barron, C.N., Martin, P.J., Smedstad, L.F., Rhodes, R.C., 2006. Validation of interannual simulations from the 1/8 degree global navy coastal ocean model (NCOM). Ocean Modelling 11, 376–398.

Lohan, M.C., Bruland, K.W., 2006. Importance of vertical mixing for additional sources of nitrate and iron to surface waters of the Columbia river plume: implications for biology. Marine Chemistry 98, 260–273.

MacCready, P., Banas, N.S., Hickey, B.M., Dever, E.P., Liu, Y., 2008. A model study of tide- and wind-induced mixing in the Columbia River estuary and plume. Continental Shelf Research, this issue, doi:10.1016/j.csr.2008.03.015.

MacFadyen, A., Hickey, B.M., Foreman, M.G.G., 2005. Transport of surface waters from the Juan de Fuca eddy region to the Washington coast. Continental Shelf Research 25, 2008–2021.

Ridderinkhof, H., Zimmerman, J.T.F., 1992. Chaotic stirring in a tidal system. Science 258, 1107–1111.

Roughan, M., Terill, E.J., Largier, J.L., Otero, M.P., 2005. Observations of divergence and upwelling around Point Loma, California. Journal of Geophysical Research 110 (C04011).

Samelson, R.M., Wiggins, S., 2006. Lagrangian Transport in Geophysical Jets and Waves: the Dynamical Systems Approach. Interdisciplinary Applied Mathematics, vol. 31. Springer, New York.

Strub, P.T., Kosro, P.M., Huyer, A., 1991. The nature of cold filaments in the California current system. Journal of Geophysical Research 96, 14,743–14,768.

Thomas, A.C., Brickley, P., 2006. Satellite measurements of chlorophyll distribution during spring 2005 in the California current. Geophysical Research Letters 33, L22S05.

Thomas, A.C., Carr, M.-E., Strub, P.T., 2001. Chlorophyll variability in eastern boundary currents. Geophysical Research Letters 28, 3421.

Umlauf, L., Burchard, H., 2003. A generic length-scale equation for geophysical turbulence models. Journal of Marine Research 61, 235–265.

Visser, A.W., 1997. Using random walk models to simulate the vertical distribution of particles in a turbulent water column. Marine Ecology Progress Series 158, 275–281.

Ware, D.M., Thomson, R.E., 2005. Bottom-up ecosystem trophic dynamics determine fish production in the northeastern Pacific. Science 308, 1280–1284.

Yankovsky, A.E., 2000. The cyclonic turning and propagation of buoyant coastal discharge along the shelf. Journal of Marine Research 58, 585–607.

Yankovsky, A.E., Hickey, B.M., Munchow, A.K., 2001. Impact of variable inflow on the dynamics of a coastal buoyant plume. Journal of Geophysical Research 106, 19,809–19,824.